

# Self-Interacting Forbidden Dark Matter under a Cannibally Co-Decaying Phase

Kwei-Chou Yang<sup>1,\*</sup>

<sup>1</sup>*Department of Physics and Center for High Energy Physics,  
Chung Yuan Christian University, 200 Chung Pei Road, Taoyuan 32023, Taiwan*

For the typical forbidden dark matter (DM), the correct relic density is determined exclusively by kinetically forbidden DM annihilations which vanish at zero temperature. We present a model that contains the DM and a heavier but unstable scalar mediator in the hidden sector. When the temperature drops below  $\sim m_{\text{DM}}$ , this hidden sector, thermally decoupled from the visible sector, enters a cannibal phase (with zero chemical potential), during which the DM density is depleted with the out-of-equilibrium decay of the scalar mediator. As such, the freeze-out process, described by forbidden DM annihilations to mediators, evolves with a temperature different from the SM bath. The DM candidate of having a mass in the range of tens of MeV can result in the correct relic density and sizable 2-to-2 self-interactions, which fit small structure problems. The future sensitivity of the NA62 beam dump experiment can probe the parameter space of the related scalar mediator.

arXiv:2306.17037v1 [hep-ph] 29 Jun 2023

---

\* [kcyang@cycu.edu.tw](mailto:kcyang@cycu.edu.tw)

## I. INTRODUCTION

While astronomical observations have strongly indicated dark matter (DM), its identity remains an open question in physics. We thus need to extend the Standard Model (SM) by including new particle(s) to account for the observed DM phenomena. However, the weak-scale DM search related to its interactions with the SM is stringently constrained by direct detection experiments, especially in the mass range  $m_{\text{DM}} \gtrsim 5$  GeV [1–4]. One exciting paradigm of models is the hidden sector DM model, for which the dark matter candidate resides within a hidden sector and communicates with the visible sector through a metastable mediator weakly coupling DM to the SM [5, 6]. This model can easily interpret the present experimental null measurements.

In this paper, we present a novel scenario where both the DM ( $X$ ) and metastable scalar mediator ( $S$ ) are bosons but with mass  $m_X < m_S$ , which reside in a hidden sector. The hidden sector is thermally decoupled from the SM bath when the temperature drops below  $\sim m_{\text{DM}}$ . After that, it enters a cannibal phase (with zero chemical potential) during which the DM density is heated but depleted with the out-of-equilibrium decay of the mediator; the former describes the number-changing interactions, called cannibalization [7, 8], while the latter is referred to as the co-decaying mechanism [9] resulting in the bath reheated. This scenario naturally leads to large self-interactions in the sub-GeV region, which may help address the ‘core vs. cusp’ and ‘too-big-to-fail’ small structure problems [10–14]. As DM annihilations are almost forbidden at temperatures of the recombination epoch, this light DM case evades the constraints from the CMB anisotropies, which are sensitive to energy injection into the intergalactic medium [15, 16].

For this class of the thermal freeze-out DM, its relic abundance is determined exclusively by forbidden channels [17–29]. We will exhibit that this mechanism does not matter whether the hidden sector is decoupled earlier from the bath at  $T \sim m_{\text{DM}}$  or later until after freeze-out. As characterized by the forbidden channel, the forbidden rate of  $XX \rightarrow SS$ , compared with its inverse process at their temperature  $T_X$ , is exponentially suppressed as

$$\langle\sigma v\rangle_{XX\rightarrow SS} \approx \langle\sigma v\rangle_{SS\rightarrow XX} \frac{g_S^2}{g_X^2} r^3 \left(1 - \frac{15\Delta}{8rx_X^2}\right) e^{-\Delta}, \quad (1)$$

where  $\Delta \equiv 2(r-1)x_X$ ,  $x_X \equiv m_X/T_X$ , the mass ratio  $r \equiv m_S/m_X > 1$ ,  $g_X$  and  $g_S$  are respectively the internal degrees of freedom of  $X$  and  $S$ .

The metastable  $S$  decays to SM particles. Supposing that the couplings between it and SM particles are still sufficiently sizable for maintaining the thermal equilibrium between the hidden sector and SM, this model describes well the critical feature of the traditional forbidden DM

scenario. For this condition, the DM freeze-out occurs at  $T = T_f$  (freeze-out temperature) below that  $\langle\sigma v\rangle_{SS\rightarrow XX} (n_S^{\text{eq}})^2 \lesssim 3Hn_X$ , where  $n_S^{\text{eq}}$  is the equilibrium density of  $S$ , and  $H$  is the Hubble parameter.

Here, we alternatively consider the parameter region where the rate of the hidden sector interactions with the SM drops below the Hubble expansion at  $T \sim m_X$  so that the hidden sector evolves with a different temperature from the SM plasma. The present scenario has the following properties:

- Interactions among the dark sector particles guarantee  $T_X = T_S$  before freeze-out.
- Below  $T \sim m_X$ , the 3-to-2 cannibal annihilations are still active. The hidden sector temperature is hotter than the SM bath as the number-changing interactions convert the mass of nonrelativistic hidden sector particles into their kinetic energy. Meanwhile, the hidden sector may cool down efficiently due to net entropy injection from the hidden sector to the SM bath, resulting from the  $S$  decaying out-of-equilibrium into the SM bath.
- During the cannibalization epoch, the hidden sector densities, following their temperature, are Boltzmann depleted and maintain chemical equilibrium (with zero chemical potential).
- When cannibalization ends, the forbidden channel described by the DM annihilation to mediators is still active and guides the evolution of hidden sector densities until freeze-out; meanwhile, 2-to-2 interactions keep hidden sector particles in temperature equilibrium but with a nonzero chemical potential.

## II. BOLTZMANN EQUATIONS AND THERMAL FREEZE-OUT

Generically, the evolutions of number densities of  $X$  and  $S$  are described by the coupled Boltzmann equations,

$$\frac{dn_X}{dt} + 3Hn_X = \{2 \leftrightarrow 2\}_{SX} - \{2 \leftrightarrow 2\}_{\text{SM}}^X + \{3 \leftrightarrow 2\}_X, \quad (2)$$

$$\begin{aligned} \frac{dn_S}{dt} + 3Hn_S = & - \left( \langle\Gamma_S\rangle_{T_i} n_S - \langle\Gamma_S\rangle_T n_S^{\text{eq}}(T) \right) \\ & - \{2 \leftrightarrow 2\}_{SX} - \{2 \leftrightarrow 2\}_{\text{SM}}^S + \{3 \leftrightarrow 2\}_S, \end{aligned} \quad (3)$$

where

$$\begin{aligned} \{2 \leftrightarrow 2\}_{SX} &\equiv \langle \sigma v \rangle_{SS \rightarrow XX}(T_i) \left( n_S^2 - \frac{(n_S^{\text{eq}}(T_i))^2}{(n_X^{\text{eq}}(T_i))^2} n_X^2 \right), \\ \{2 \leftrightarrow 2\}_{\text{SM}}^X &\equiv \langle \sigma v \rangle_{XX \rightarrow \text{SM SM}}(T_i) n_X^2 \\ &\quad - \langle \sigma v \rangle_{XX \rightarrow \text{SM SM}}(T) (n_X^{\text{eq}}(T))^2, \end{aligned}$$

$\{2 \leftrightarrow 2\}_{\text{SM}}^S$  is the same as  $\{2 \leftrightarrow 2\}_{\text{SM}}^X$  but with  $X$  replaced by  $S$ ,  $n_{X,S}^{\text{eq}}(T_i)$  are the equilibrium densities at temperature  $T_i$ ,  $\langle \Gamma_S \rangle$  is the thermally averaged width of  $S$ ,  $\{3 \leftrightarrow 2\}_{X,S}$  denote terms involving  $3 \leftrightarrow 2$  number-changing interactions (see Appendix A and also [26, 30] for a detailed expression). Here,  $T_i \equiv T_X$ , but if the hidden sector particles are in thermal equilibrium with the SM bath during the freeze-out process, we have  $T_i \equiv T_X = T$ , the same as the bath temperature.

For Eq. (2), first considering the condition  $T_i \equiv T_X = T$  that the hidden sector particles are in temperature equilibrium among themselves and also with the SM bath during the freeze-out process, the evolution of the DM number density can be approximately described by

$$\frac{dY_X}{dx} \approx - \frac{s \langle \sigma v \rangle_{SS \rightarrow XX} (Y_S^{\text{eq}})^2}{xH (Y_X^{\text{eq}})^2} \left[ Y_X^2 - (Y_X^{\text{eq}})^2 \right], \quad (4)$$

where  $Y_{X,S} \equiv n_{X,S}/s$ ,  $Y_{X,S}^{\text{eq}} \equiv n_{X,S}^{\text{eq}}(T)/s$ , the Universe's total entropy density is  $s = (2\pi^2/45)h_{\text{eff}}T^3$ , and  $x \equiv m_X/T$ . Analogous to the calculation of the WIMP (weak interacting massive particle) DM, for the s-wave  $SS \leftrightarrow XX$  annihilation, one can obtain the following results

$$\frac{x_f^{\frac{1}{2}} e^{(2r-1)x_f}}{\langle \sigma v \rangle_{SS \rightarrow XX}} \approx \delta(\delta + 2) \sqrt{\frac{45}{4\pi^5}} \frac{M_{\text{pl}} m_X r^3 g_S^2}{g_{\text{eff}}^{1/2}(T_f) g_X}, \quad (5)$$

$$\begin{aligned} \frac{1}{m_X Y_X^\infty} &\approx \frac{4\pi}{\sqrt{90}} M_{\text{pl}} g_*^{1/2}(T_f) \langle \sigma v \rangle_{SS \rightarrow XX} \frac{g_S^2}{g_X^2} r^3 \\ &\quad \times \left\{ \frac{e^{-\Delta_f}}{x_f} + \frac{\Delta_f}{x_f} \text{Ei}(-\Delta_f) - \frac{15}{8} \left( 1 - \frac{1}{r} \right) \right. \\ &\quad \left. \times \left[ \frac{1 - \Delta_f}{x_f^2} e^{-\Delta_f} - \frac{\Delta_f^2}{x_f^2} \text{Ei}(-\Delta_f) \right] \right\}, \quad (6) \end{aligned}$$

where  $M_{\text{pl}} \equiv (8\pi G)^{-1/2}$  is the reduced Planck mass,  $\delta \sim 1$  is defined by  $Y_X - Y_X^{\text{eq}} = \delta Y_X^{\text{eq}}$  with  $d\delta/dx \ll 1$ ,  $\Delta_f \equiv 2(r-1)x_f$ ,  $\text{Ei}(z) = -\int_{-z}^{\infty} (e^{-t}/t) dt$ , and  $Y_X^\infty$  is the post-freeze-out value of the yield, related to the DM relic abundance [31]  $\Omega_X = m_X Y_X^\infty s_0 / \rho_c \simeq 0.1198/h^2$  with the present critical density  $\rho_c = 1.0537 \times 10^{-5} h^2 (\text{GeV}/c^2) \text{cm}^{-3}$ ,  $h \simeq 0.674$ , and the present entropy  $s_0 = 2891 \text{ cm}^{-3}$ .

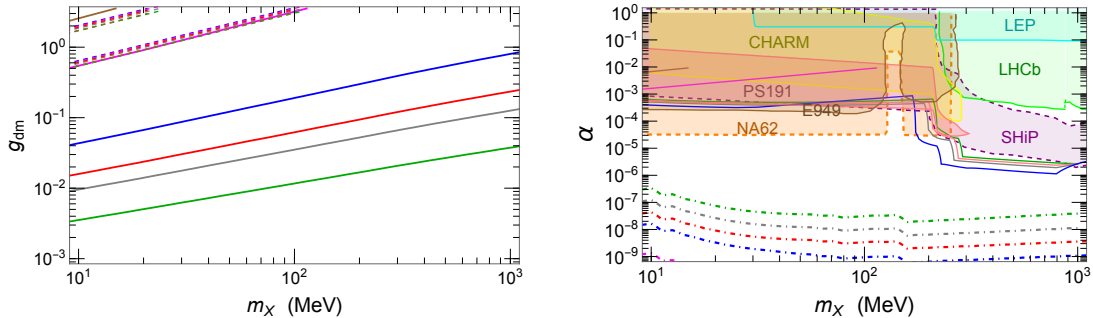


FIG. 1. Left panel:  $g_{\text{dm}}$  as a function of  $m_X$ , that can produce the correct relic density (solid lines) and approximate the current self-interactions  $\sigma_{\text{SI}}/m_X \in (0.1, 10) \text{ cm}^2/g$  (within the region bounded by dashed lines). Right panel: (a) The solid lines show the lower bound of  $\alpha$  about keeping the hidden sector in temperature equilibrium with the bath before freeze-out. (b) Dashed lines show the minimum  $\alpha$  above that  $Y_{X,S}$  grow by up to  $Y_{X,S}^{\text{eq}}(T)$  at  $T \gtrsim m_X$  by a freeze-in process. (c) colored regions with solid boundaries are excluded by experiments denoted [33–37], while that with dashed boundaries indicate sensitivity projections [38–41], where for simplicity  $r = 1.01$  is used. The green, gray, red, blue, magenta, and brown lines correspond to  $r(= m_S/m_X) = 1.01, 1.1, 1.5, 1.25, 1.5$ , and  $1.65$ , respectively. The unitarity bound  $g_{\text{dm}} < \sqrt{4\pi}$  is imposed.

### III. MODEL

We take the simplest renormalizable vector dark matter model [30, 32] as an example to illustrate the pictures discussed. The covariant derivative of the dark sector is given by  $D_\mu \Phi_S \equiv (\partial_\mu + ig_{\text{dm}} Q_X X_\mu) \Phi_S$ . The  $Z_2$  symmetry,  $X_\mu \rightarrow -X_\mu$  and  $\Phi_S \rightarrow \Phi_S^*$ , is imposed to the Lagrangian for stabilizing the DM,  $X_\mu$ , which (denoted as  $X$  throughout this paper) is the abelian gauge vector boson of a dark  $U(1)_X$ . The scalar potentials of the Lagrangian are given by

$$\begin{aligned} \mathcal{L}_{\text{hidden}} = & -\mu_H^2 |\Phi_H|^2 - \mu_S^2 |\Phi_S|^2 - \frac{\lambda_H}{2} (\Phi_H^\dagger \Phi_H)^2 \\ & - \frac{\lambda_S}{2} (\Phi_S^\dagger \Phi_S)^2 - \lambda_{HS} (\Phi_H^\dagger \Phi_H) (\Phi_S^\dagger \Phi_S), \end{aligned} \quad (7)$$

where  $\Phi_H = (H^+, H^0)$  is the SM Higgs doublet. Two neutral Higgs fields are parametrized as  $H^0 = \frac{1}{\sqrt{2}}(v_H + \phi_h + i\sigma_h)$  and  $\Phi_S = \frac{1}{\sqrt{2}}(v_S + \phi_s + i\sigma_s)$ , which are related to the mass eigenstates,  $h = \cos \alpha \phi_h + \sin \alpha \phi_s$ ,  $S = -\sin \alpha \phi_h + \cos \alpha \phi_s$ . The dark matter gets its mass,  $m_X = g_{\text{dm}} Q_X v_S$ , from the vacuum expectation value of the hidden scalar through the spontaneous symmetry breaking, and  $\sigma_s$  becomes its longitudinal component. We use the dark charge  $Q_X = 1$  in the analysis.

Using this model and the combination of Eqs. (5) and (6), in the left panel of Fig. 1, we show the coupling strength  $g_{\text{dm}}$  that accounts for the observed relic density. Under the condition that

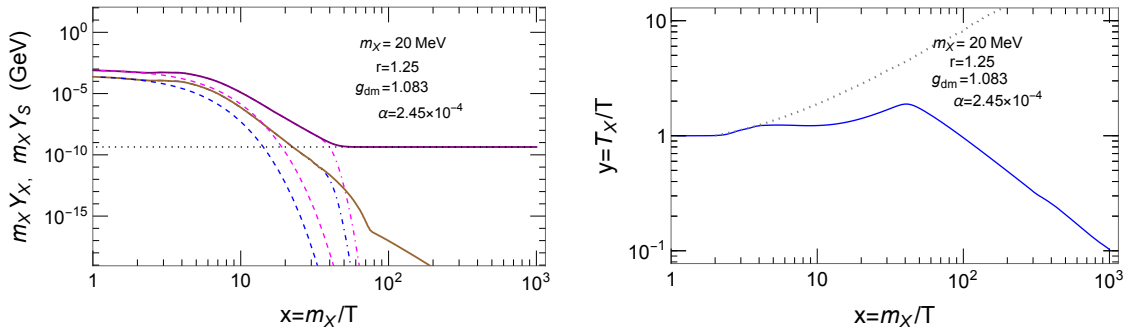


FIG. 2. Left panel:  $m_X Y_X$  (solid purple line) and  $m_X Y_S$  (solid brown line) as functions of  $x$ . The magenta and blue dashed lines (or dot-dashed lines) depict the corresponding ones following Boltzmann suppression with  $T$  (or their temperature  $T_X$ ). The value of  $g_{\text{dm}}$  gives  $\sigma_{\text{SI}}/m_X = 0.1 \text{ cm}^2/g$ . The horizontal dotted line denotes the correct DM relic abundance. Right panel:  $y$  vs.  $x$  (blue curve). After decoupling, if the entropy is separately conserved in the hidden sector and SM, the temperature ratio instead follows the dashed line.

can keep the hidden sector and the bath in the thermal equilibrium until after freeze-out, via elastic ( $X \text{ SM} \leftrightarrow X \text{ SM}$  and  $S \text{ SM} \leftrightarrow S \text{ SM}$ ) and number-changing ( $S \leftrightarrow \text{SM SM}$ ) interactions, in the right panel, we display the corresponding lowest value of  $\alpha$ . For the same condition, the correct relic abundance mainly depends on the values of  $m_X, m_S/m_X$  and  $g_{\text{dm}}$ , but is insensitive to  $\alpha$ . The experimental bounds are summarized in Fig. 1. The SHiP experiment [38, 39] can explore most remaining parameter space (see also Fig. 3).

We also show the minimum  $\alpha$ , denoted as the dot-dashed lines in the right panel and  $\alpha_{\text{fi}}$  below, that can result in the hidden sector particles arriving at their equilibrium density at  $T \gtrsim m_X$  through a freeze-in process mainly via interactions  $\text{SM SM} \rightarrow SS$  and  $\text{SM SM} \rightarrow S$ . Because  $Y_S(T) \gtrsim Y_X(T)$  during freeze-in, and, meanwhile, the hidden sector quickly reaches its internal thermal equilibrium through interactions  $XX \leftrightarrow SS$  and  $XS \leftrightarrow XS$ , we thus estimate  $\alpha_{\text{fi}}$ : via the freeze-in  $Y_S^{\text{eq}}(m_X) \simeq \int_0^{Y_S^{\text{eq}}(m_X)} dY_S$ , given by

$$Y_S^{\text{eq}}(m_X) \simeq \int_0^1 \frac{\tilde{h}_{\text{eff}} s \langle \sigma v \rangle_{SS \rightarrow \text{SM SM}} Y_S^{\text{eq}2} + \langle \Gamma_S \rangle Y_S^{\text{eq}}}{h_{\text{eff}} x H} dx, \quad (8)$$

where  $\tilde{h}_{\text{eff}} \equiv h_{\text{eff}} [1 + (1/3)(d \ln h_{\text{eff}}/d \ln T)]$ , and the value of  $g_{\text{dm}}$  that can account for the correct relic density is used in the coupling  $g_{SSS} \sim -3 \cos^3 \alpha m_S^2 g_{\text{dm}}/m_X$  [26] when evaluating the  $SS \rightarrow \text{SM SM}$  cross section. Fig. 1 shows that thermal freeze-out forbidden dark matter can be produced from an initial null abundance.

The DM self-interacting cross section obeying  $\sigma_{\text{SI}}/m_X \in (0.1, 10) \text{ cm}^2/g$  is shown by the region bounded by dashed lines in the left panel of Fig. 1. For the case that the hidden sector is in

temperature equilibrium with the SM bath until after freeze-out, to have a much larger self-interacting cross section, the mass ratio needs to be in the range  $1.5 < m_S/m_X < 1.65$ . However, this parameter region is excluded by E949, PS191, and CHARM measurements [33–35].

#### IV. CANNIBALLY CO-DECAYING PHASE

Alternatively, as the hidden sector is chemically decoupled from the bath earlier at  $T \sim m_X$ , in Fig. 2 we numerically illustrate the typical thermal evolution of the self-interacting forbidden DM under a cannibally co-decaying phase. Here, the decoupling temperature is  $T \simeq 10$  MeV. After that, if there is no net entropy flow between the hidden sector and SM, their entropy ratio is fixed, and the temperature ratio will evolve as the dashed line denoted in the right panel. In reality, because  $S$  decays out-of-equilibrium, resulting in net entropy injection from the hidden sector to the bath, the SM bath is reheated. The total comoving entropy  $S_t$  of the Universe is increased as

$$dS_t = \left( \frac{1}{T} - \frac{1}{T_X} \right) a^3 dt \Gamma_{SmS} (n_S - n_S^{\text{eq}}(T)), \quad (9)$$

where  $a$  is the comoving scale factor. As such, the time derivative rewritten in terms of the bath temperature is

$$\frac{d}{dt} = (1 - \delta_t) x H \frac{h_{\text{eff}}(T)}{\tilde{h}_{\text{eff}}(T)} \frac{d}{dx}, \quad (10)$$

where  $\delta_t \equiv rx\Gamma_S(Y_S - Y_S^{\text{eq}}(T))(1 - y^{-1})/(3H)$  with  $y \equiv T_X/T$ . The detailed Boltzmann equations are collected in Appendix A. In this scenario, the hidden sector particles' temperature, compared with the SM bath, is heated by cannibalization, which results in larger thermal equilibrium densities since they evolve with  $T_X$  instead of  $T$ . From Eq. (2), letting  $T_i \equiv T_X$ , i.e., the hidden sector evolving with an independent temperature, and using  $x_h \equiv m_X/T_X$  as the variable, the DM evolution can be approximated by

$$\begin{aligned} \frac{dY_X}{dx_h} &\approx - \frac{s}{x_h H (1 - \delta_t)} \left( 1 - \frac{d \log y}{d \log x} \right)^{-1} \langle \sigma v \rangle_{SS \rightarrow XX} \\ &\times \frac{(Y_S^{\text{eq}}(T_X))^2}{(Y_X^{\text{eq}}(T_X))^2} \left( Y_X^2 - (Y_X^{\text{eq}}(T_X))^2 \right). \end{aligned} \quad (11)$$

We therefore obtain the same results as Eqs. (5) and (6) but with replacement:  $x_f \rightarrow x_h^f \equiv m_X/T_X^f$  and  $\langle \sigma v \rangle_{SS \rightarrow XX} \rightarrow [(1 - \delta_t)(1 - \frac{d \log y}{d \log x})]^{-1} \langle \sigma v \rangle_{SS \rightarrow XX}$ , where  $T_X^f$  is the freeze-out temperature of DM. As a result, a much larger  $g_{\text{dm}}$  is required to delay the freeze-out time, such that the DM co-decays with the out-of-equilibrium decay of the mediator and its density can be sufficiently depleted to account for the observed relic density. Thus, we could expect a sizable DM self-interaction cross

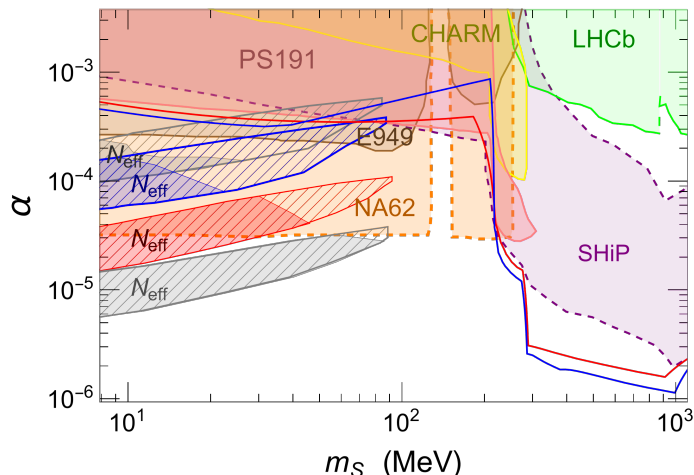


FIG. 3. Constraints on the  $(m_S, \alpha)$  parameter space in the sub-GeV region. For freeze-out forbidden DM with  $r = 1.25$  (1.15) under a cannibally co-decaying phase, using a value of  $g_{\text{dm}}$  that leads to observations bounded by  $\sigma_{\text{SI}}/m_X \in (0.1, 10) \text{ cm}^2/g$ , the blue (red) hatched area produces the correct relic density, where the shaded region in the same color is excluded by the Planck constraint on  $N_{\text{eff}}$  at  $2\sigma$ . Moreover, for comparison the upper (lower) gray region is for  $r = 1.3$  (1.1). Others are the same as the right panel of Fig. 1.

section  $\sigma_{\text{SI}}$  due to having a much larger  $g_{\text{dm}}$ . As shown in Fig. 2, imposing  $g_{\text{dm}} = 1.083$ , which leads to the correct relic density, indeed results in a sizable  $\sigma_{\text{SI}}/m_X = 0.1 \text{ cm}^2/g$ . The formula for  $\sigma_{\text{SI}}$  is given in Appendix B.

Although the N-body simulation using the collisionless cold DM scenario can successfully describe the Universe's large-scale structure, its predictions exist inconsistencies in small-scale observations of galaxy formations. Sizable DM self-interactions, which the forbidden dark matter can account for under a cannibally co-decaying phase, alleviate such tensions at a small scale, for instance, core-cusp and too-big-to-fail problems.

## V. PHENOMENOLOGY AND CONCLUSIONS

The present framework gives velocity-independent self-interaction cross-sections in the zero temperature limit. Using the value of  $g_{\text{dm}}$  constrained by observations with the strength  $\sigma_{\text{SI}}/m_X \in (0.1, 10) \text{ cm}^2/g$  [10–14], we show the region (blue hatched) in Fig. 3 that can account for the correct relic density.

The unstable light scalar, which resides within a hidden sector and is the partner of the for-

bidden DM, could be produced in rare decays performed at colliders and fixed target experiments. Fig. 3 shows the constraints on the parameter space of the unstable scalar in the sub-GeV region. Finding the long-lived scalar particle at beam dump experiments with detectors far from the event generation is promising. It is likely to discover the signal hint for the self-interacting forbidden DM through the future NA62 beam dump experiment.

In the mass range of interest (*e.g.* the hatched regions in Fig. 3), the DM freeze-out occurs after the neutrinos have decoupled (see also Fig. 2). Once  $S$  decays out-of-equilibrium to photons after neutrino decoupling, the photon bath is further heated relative to neutrinos, thereby reducing the effective extra number of relativistic species,

$$N_{\text{eff}} = \frac{8}{7} \left( \frac{11}{4} \right)^{4/3} \frac{3\rho_\nu}{\rho_\gamma + \delta\rho_\gamma} \Big|_{T=T_{\text{dec}}} . \quad (12)$$

We approximate the extra injection energy to the bath due to the hidden sector particles as  $\delta\rho_\gamma \approx (\rho_S + \rho_X)_{T=T_{\text{dec}}}$  with  $T_{\text{dec}} = 1$  MeV used. Combining with baryon acoustic oscillation (BAO), Planck 2018 constrains  $N_{\text{eff}} = 2.99 \pm 0.17$  [42]. Using the SM value  $N_{\text{eff}}^{\text{SM}} = 3.046$  [43], we limit  $\Delta N_{\text{eff}} = N_{\text{eff}} - N_{\text{eff}}^{\text{SM}} \gtrsim -0.396$  at  $2\sigma$ , resulting in the requirement of  $m_S Y_S + m_X Y_X \lesssim 1.9 \times 10^{-5}$  GeV at  $T_{\text{dec}}$ . This constraint, shown in Fig. 3, can rule out some parameter regions with  $m_S \lesssim 10$  MeV. Note that for  $T \lesssim m_X$  because the hidden sector particles, following their temperatures, are still Boltzmann suppressed, the results are not constrained by the big bang nucleosynthesis.  $\Delta N_{\text{eff}}$  and E949 can further constrain the mass ratio to lie in the range  $1.1 \lesssim r (= m_S/m_X) \lesssim 1.33$  and the scalar mass to be  $8 \text{ MeV} \lesssim m_S \lesssim 100 \text{ MeV}$ . Moreover, the nearly favored parameter space is projected to be testable with the NA62 experiment.

In conclusion, we have proposed the self-interacting forbidden dark matter framework under a cannibally co-decaying phase. The DM candidate of having a mass in the range of tens of MeV can result in the correct relic density and sizable 2-to-2 self-interactions, which fit small structure problems. The projected sensitivity of the NA62 beam dump experiment can probe the parameter space of the related scalar mediator.

**Acknowledgments.** This work was partly supported by the National Center for Theoretical Sciences and the National Science and Technology Council of Taiwan under grant number MOST 111-2112-M-033-006.

### Appendix A: Boltzmann equations

We consider a dark matter candidate that resides within a hidden sector and interacts with the SM particles through a heavier and unstable scalar  $S$ . Meanwhile, the dark sector particles are in thermal equilibrium, i.e.,  $T_X = T_S$ , before freeze-out. If the scalar with temperature  $T_X$  decays out-of-equilibrium into relativistic thermalized SM particles with temperature  $T$ , following the second law of thermodynamics, the total comoving entropy,  $S_t$ , is increased and given by the revised form,

$$\begin{aligned} dS_t &= d(sa^3) = \frac{dQ}{T} - \frac{dQ}{T_X} \\ &= \left( \frac{1}{T} - \frac{1}{T_X} \right) a^3 dt \Gamma_S m_S (n_S - n_S^{\text{eq}}(T)) , \end{aligned} \quad (\text{A1})$$

where  $n_S^{\text{eq}}(T)$  is the equilibrium density of the scalar  $S$  at the bath temperature  $T$ ,  $dQ$  is the net heat transferred from the hidden scalar to the SM bath, described by

$$\begin{aligned} dQ &= -d(a^3 \rho_S) = -a^3 dt \left( \dot{\rho}_S + 3 \frac{\dot{a}}{a} \rho_S \right) \\ &= a^3 dt \Gamma_S m_S (n_S - n_S^{\text{eq}}(T)) , \end{aligned} \quad (\text{A2})$$

and  $a$  is the cosmic scale factor. Here, the total entropy density of the Universe is

$$s = \frac{2\pi^2}{45} h_{\text{eff}}(T) T^3 , \quad (\text{A3})$$

where the effective number of the total degrees of freedom is given by

$$h_{\text{eff}}(T) = h_{\text{eff}}^{\text{SM}}(T) + (h_{\text{eff}}^X(T_X) + h_{\text{eff}}^S(T_X)) \left( \frac{T_X}{T} \right)^3 \quad (\text{A4})$$

with

$$h_{\text{eff}}^i(T_X) = \frac{45g_i}{4\pi^4} \left( \frac{m_i}{T_X} \right)^4 \int_1^\infty \frac{y(y^2 - 1)^{1/2} 4y^2 - 1}{e^{m_i y/T_X} - 1} \frac{dy}{3y} , \quad (\text{A5})$$

and  $i \equiv X$  or  $S$  for the DM or hidden scalar. Including the effect that the total comoving entropy could be changed due to the out-of-equilibrium decay of the hidden scalar and considering that the temperature decoupling of  $S$  and  $X$  occurs until after freeze-out, we can then deduce the time derivative in terms of the bath temperature,

$$\begin{aligned} \frac{d}{dt} &= \frac{ds}{dt} \frac{dT}{ds} \frac{d}{dT} = \left[ \frac{1}{3s} \Gamma_S m_S (n_S - n_S^{\text{eq}}(T)) (1 - y^{-1}) - HT \right] \frac{h_{\text{eff}}(T)}{\tilde{h}_{\text{eff}}(T)} \frac{d}{dT} \\ &= (1 - \delta_t) x H \frac{h_{\text{eff}}(T)}{\tilde{h}_{\text{eff}}(T)} \frac{d}{dx} , \end{aligned} \quad (\text{A6})$$

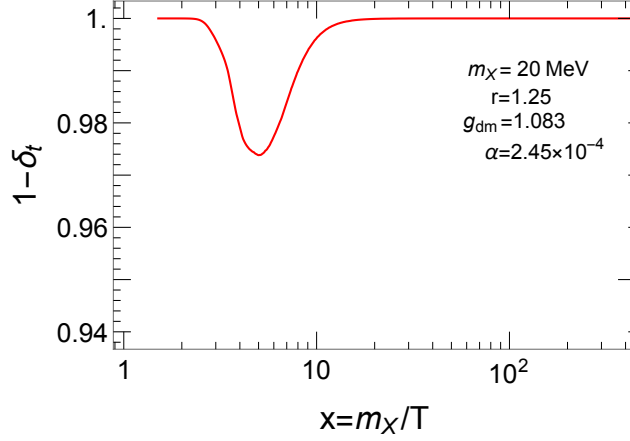


FIG. 4. An additional factor  $1 - \delta_t$  is needed to translate the time scale to the temperature parameter  $x$ . This is due to the increase of the total comoving entropy resulting from the out-of-equilibrium decay of the scalar  $S$ .

where  $x = m_X/T$  is the dimensionless temperature variable,  $H = [(8\pi/3)G_N\rho]^{1/2}$  is the Hubble parameter with  $\rho$  the total energy density of the Universe, and

$$\delta_t \equiv \frac{1}{3H} x \frac{m_S}{m_X} \Gamma_S (Y_S - Y_S^{\text{eq}}(T_X)) (1 - y^{-1}). \quad (\text{A7})$$

In Fig. 4, we show the relative factor  $1 - \delta_t$ , which results from the increase of the total comoving entropy.

Here and through this paper, we have introduced dimensionless quantities,

$$Y_X \equiv \frac{n_X}{s}, \quad Y_S \equiv \frac{n_S}{s}, \quad (\text{yields})$$

$$y = \frac{T_X}{T}, \quad (\text{temperature ratio}) \quad (\text{A8})$$

as functions of a dimensionless variable  $x$  and  $Y_k^{\text{eq}}(T_\ell) \equiv n_k^{\text{eq}}(T_\ell)/s(T)$ , with the subscript  $k \equiv X, S$  and  $T_\ell = T_X, T$ . We obtain the coupled Boltzmann equations of the yields,

$$\begin{aligned} \frac{dY_X}{dx} = & (1 - \delta_t)^{-1} \frac{\tilde{h}_{\text{eff}}(T)}{h_{\text{eff}}(T)} \frac{1}{xH} \\ & \times \left[ 3H\delta_t Y_X + s\langle\sigma v\rangle_{SS\rightarrow XX}(T_X) \left( Y_S^2 - \frac{(Y_S^{\text{eq}}(T_X))^2}{(Y_X^{\text{eq}}(T_X))^2} Y_X^2 \right) \right. \\ & + \frac{s^2}{3} \langle\sigma v^2\rangle_{SS\rightarrow XX} \left( Y_S^3 - \frac{(Y_S^{\text{eq}}(T_X))^3}{(Y_X^{\text{eq}}(T_X))^2} Y_X^2 \right) - s^2 \langle\sigma v^2\rangle_{XXS\rightarrow SS} \left( Y_X^2 Y_S - \frac{(Y_X^{\text{eq}}(T_X))^2}{Y_S^{\text{eq}}(T_X)} Y_S^2 \right) \\ & - \frac{s^2}{3} \langle\sigma v^2\rangle_{XX\rightarrow XS} \left( Y_X^3 - \frac{(Y_X^{\text{eq}}(T_X))^2}{Y_S^{\text{eq}}(T_X)} Y_X Y_S \right) \\ & \left. - s \left( \langle\sigma v\rangle_{XX\rightarrow\sum_{ij} \text{SM}_i \text{SM}_j}(T_X) Y_X^2 - \langle\sigma v\rangle_{XX\rightarrow\sum_{ij} \text{SM}_i \text{SM}_j}(T) (Y_X^{\text{eq}}(T))^2 \right) \right], \quad (\text{A9}) \end{aligned}$$

$$\begin{aligned}
\frac{dY_S}{dx} = & (1 - \delta_t)^{-1} \frac{\tilde{h}_{\text{eff}}(T)}{h_{\text{eff}}(T)} \frac{1}{xH} \\
& \times \left[ 3H\delta_t Y_S - s\langle\sigma v\rangle_{SS\rightarrow XX}(T_X) \left( Y_S^2 - \frac{(Y_S^{\text{eq}}(T_X))^2}{(Y_X^{\text{eq}}(T_X))^2} Y_X^2 \right) \right. \\
& - \Gamma_S \left( \frac{K_1(m_S/T_X)}{K_2(m_S/T_X)} Y_S - \frac{K_1(m_S/T)}{K_2(m_S/T)} Y_S^{\text{eq}}(T) \right) \\
& - s \left( \langle\sigma v\rangle_{SS\rightarrow\sum_{ij} \text{SM}_i \text{SM}_j}(T_X) Y_S^2 - \langle\sigma v\rangle_{SS\rightarrow\sum_{ij} \text{SM}_i \text{SM}_j}(T) (Y_S^{\text{eq}}(T))^2 \right) \\
& + \frac{s^2}{6} \langle\sigma v^2\rangle_{XXX\rightarrow XS} \left( Y_X^3 - Y_X Y_S \frac{(Y_X^{\text{eq}}(T_X))^2}{Y_S^{\text{eq}}(T_X)} \right) - \frac{s^2}{6} \langle\sigma v^2\rangle_{SSS\rightarrow SS} \left( Y_S^3 - Y_S^2 Y_S^{\text{eq}}(T_X) \right) \\
& + \frac{s^2}{2} \langle\sigma v^2\rangle_{XXS\rightarrow SS} \left( Y_X^2 Y_S - \frac{(Y_X^{\text{eq}}(T_X))^2}{Y_S^{\text{eq}}(T_X)} Y_S^2 \right) - \frac{s^2}{2} \langle\sigma v^2\rangle_{SSS\rightarrow XX} \left( Y_S^3 - \frac{(Y_S^{\text{eq}}(T_X))^3}{(Y_X^{\text{eq}}(T_X))^2} Y_X^2 \right) \\
& \left. - \frac{s^2}{2} \langle\sigma v^2\rangle_{XSS\rightarrow XS} \left( Y_X Y_S^2 - Y_X Y_S Y_S^{\text{eq}}(T_X) \right) \right], \tag{A10}
\end{aligned}$$

and the evolution of the temperature ratio,

$$\begin{aligned}
\frac{dy}{dx} = & \frac{y}{x} - 3 \frac{\delta_t}{1 - \delta_t} \frac{\tilde{h}_{\text{eff}}(T)}{h_{\text{eff}}(T)} \frac{y}{x} - \frac{y}{Y_X + Y_S} \left( \frac{dY_X}{dx} + \frac{dY_S}{dx} \right) \\
& + \frac{(1 - \delta_t)^{-1} \tilde{h}_{\text{eff}}(T)}{Y_X + Y_S} \left\{ - (2 - \delta_H^X) \left( \frac{y}{x} + \frac{\gamma_X}{xH} (y - 1) \right) Y_X \right. \\
& - \frac{s}{xH} \left( y Y_X^2 \langle\widetilde{\sigma v}\rangle_{XX\rightarrow\sum_{ij} \text{SM}_i \text{SM}_j}(T_X) - (Y_X^{\text{eq}}(T))^2 \langle\widetilde{\sigma v}\rangle_{XX\rightarrow\sum_{ij} \text{SM}_i \text{SM}_j}(T) \right) \\
& + \frac{s^2}{m_X H} \left[ \frac{(4m_X^2 - m_S^2)(16m_X^2 - m_S^2)}{108m_X(10m_X^2 - m_S^2)} \langle\sigma v^2\rangle_{XXX\rightarrow XS} \left( Y_X^3 - \frac{Y_X Y_S (Y_X^{\text{eq}}(T_X))^2}{Y_S^{\text{eq}}(T_X)} \right) \right. \\
& + \frac{m_S^2(2m_X + m_S)(2m_X + 3m_S)}{4(m_X + 2m_S)(2m_X^2 + 4m_X m_S + 3m_S^2)} \langle\sigma v^2\rangle_{XSS\rightarrow XS} \left( Y_X Y_S^2 - Y_X Y_S Y_S^{\text{eq}}(T_X) \right) \\
& \left. + \frac{(2m_X + 3m_S)(3m_S - 2m_X)}{54m_S} \langle\sigma v^2\rangle_{SSS\rightarrow XX} \left( Y_S^3 - \frac{Y_X^2 (Y_S^{\text{eq}}(T_X))^3}{(Y_X^{\text{eq}}(T_X))^2} \right) \right] \\
& - (2 - \delta_H^S) \left( \frac{y}{x} + \frac{\gamma_S}{xH} (y - 1) \right) Y_S \\
& - \frac{s}{xH} \left( y Y_S^2 \langle\widetilde{\sigma v}\rangle_{SS\rightarrow\sum_{ij} \text{SM}_i \text{SM}_j}(T_X) - (Y_S^{\text{eq}}(T))^2 \langle\widetilde{\sigma v}\rangle_{SS\rightarrow\sum_{ij} \text{SM}_i \text{SM}_j}(T) \right) \\
& - \frac{\Gamma_S}{xH} \left( \frac{K_1(m_S/T_X)}{K_2(m_S/T_X)} Y_S \delta_\Gamma(T_X) y - \frac{K_1(m_S/T)}{K_2(m_S/T)} Y_S^{\text{eq}}(T) \delta_\Gamma(T) \right) \\
& + \frac{s^2}{m_X H} \left[ \frac{(4m_X^2 - m_S^2)(16m_X^2 - m_S^2)}{108m_X(8m_X^2 + m_S^2)} \langle\sigma v^2\rangle_{XXX\rightarrow XS} \left( Y_X^3 - \frac{Y_X Y_S (Y_X^{\text{eq}}(T_X))^2}{Y_S^{\text{eq}}(T_X)} \right) \right. \\
& + \frac{(2m_X + 3m_S)(2m_X - m_S)}{6(2m_X + m_S)} \langle\sigma v^2\rangle_{XXS\rightarrow SS} \left( Y_X^2 Y_S - \frac{Y_S^2 (Y_X^{\text{eq}}(T_X))^2}{Y_S^{\text{eq}}(T_X)} \right) \\
& + \frac{m_S(2m_X + m_S)(2m_X + 3m_S)}{4(m_X + 2m_S)(4m_X + 5m_S)} \langle\sigma v^2\rangle_{XSS\rightarrow XS} \left( Y_X Y_S^2 - Y_X Y_S Y_S^{\text{eq}}(T_X) \right) \\
& \left. + \frac{5}{54} m_S \langle\sigma v^2\rangle_{SSS\rightarrow SS} \left( Y_S^3 - Y_S^2 Y_S^{\text{eq}}(T_X) \right) \right] \left. \right\}, \tag{A11}
\end{aligned}$$

where we have the notations:  $\langle \widetilde{\sigma v} \rangle_{SS \rightarrow \sum_{ij} \text{SM}_i \text{SM}_j}(T_\ell) \equiv \langle \sigma v \cdot \frac{\mathbf{p}_S^2}{3E_S} \rangle_{SS \rightarrow \sum_{ij} \text{SM}_i \text{SM}_j}(T_\ell)/T_\ell$ , with the subscript  $k \equiv X, S$  and  $T_\ell = T_X, T$ . More interpretations for the notations can be found in Refs. [26, 30].

### Appendix B: The self-interaction cross section of the dark matter

In the zero-velocity limit of the incoming particles, the cross section for the self-interacting DM scattering  $XX \rightarrow XX$  through the scalar mediator exchange via  $s$ -,  $u$ -, and  $t$ -channels is given by (with  $c_\alpha \equiv \cos \alpha$ )

$$\sigma_{\text{SI}} = \frac{c_\alpha^4 g_{\text{dm}}^4 m_X^2 (32m_X^4 - 24m_X^2 m_S^2 + 7m_S^4 + 2m_S^2 \Gamma_S^2)}{96m_S^4 \left( (4m_X^2 - m_S^2)^2 + m_S^2 \Gamma_S^2 \right) \pi}. \quad (\text{B1})$$

- 
- [1] E. Aprile *et al.* [XENON], Phys. Rev. Lett. **121** (2018) no.11, 111302 [arXiv:1805.12562 [astro-ph.CO]].
  - [2] Y. Meng *et al.* [PandaX-4T], Phys. Rev. Lett. **127** (2021) no.26, 261802 [arXiv:2107.13438 [hep-ex]].
  - [3] E. Aprile *et al.* [XENON], Phys. Rev. Lett. **122** (2019) no.14, 141301 [arXiv:1902.03234 [astro-ph.CO]].
  - [4] D. S. Akerib *et al.* [LUX-ZEPLIN Collaboration], arXiv:1802.06039 [astro-ph.IM].
  - [5] M. Pospelov, A. Ritz and M. B. Voloshin, Phys. Lett. B **662**, 53-61 (2008) [arXiv:0711.4866 [hep-ph]].
  - [6] A. Berlin, D. Hooper and G. Krnjaic, Phys. Rev. D **94**, no.9, 095019 (2016) doi:10.1103/PhysRevD.94.095019 [arXiv:1609.02555 [hep-ph]].
  - [7] E. D. Carlson, M. E. Machacek and L. J. Hall, Astrophys. J. **398**, 43-52 (1992)
  - [8] M. Farina, D. Pappadopulo, J. T. Ruderman and G. Trevisan, JHEP **12**, 039 (2016) [arXiv:1607.03108 [hep-ph]].
  - [9] J. A. Dror, E. Kuflik and W. H. Ng, Phys. Rev. Lett. **117**, no.21, 211801 (2016) [arXiv:1607.03110 [hep-ph]].
  - [10] R. Dave, D. N. Spergel, P. J. Steinhardt and B. D. Wandelt, Astrophys. J. **547**, 574-589 (2001) [arXiv:astro-ph/0006218 [astro-ph]].
  - [11] M. Vogelsberger, J. Zavala and A. Loeb, Mon. Not. Roy. Astron. Soc. **423**, 3740 (2012) [arXiv:1201.5892 [astro-ph.CO]].
  - [12] M. Rocha, A. H. G. Peter, J. S. Bullock, M. Kaplinghat, S. Garrison-Kimmel, J. Onorbe and L. A. Moustakas, Mon. Not. Roy. Astron. Soc. **430**, 81-104 (2013) [arXiv:1208.3025 [astro-ph.CO]].
  - [13] A. H. G. Peter, M. Rocha, J. S. Bullock and M. Kaplinghat, Mon. Not. Roy. Astron. Soc. **430**, 105 (2013) [arXiv:1208.3026 [astro-ph.CO]].
  - [14] J. Zavala, M. Vogelsberger and M. G. Walker, Mon. Not. Roy. Astron. Soc. **431**, L20-L24 (2013) doi:10.1093/mnrasl/sls053 [arXiv:1211.6426 [astro-ph.CO]].
  - [15] T. R. Slatyer, Phys. Rev. D **93**, no.2, 023527 (2016) [arXiv:1506.03811 [hep-ph]].

- [16] T. R. Slatyer, Phys. Rev. D **93**, no.2, 023521 (2016) [arXiv:1506.03812 [astro-ph.CO]].
- [17] K. Griest and D. Seckel, Phys. Rev. D **43** (1991), 3191-3203
- [18] S. Tulin, H. B. Yu and K. M. Zurek, Phys. Rev. D **87** (2013) no.3, 036011 [arXiv:1208.0009 [hep-ph]].
- [19] C. B. Jackson, G. Servant, G. Shaughnessy, T. M. P. Tait and M. Taoso, JCAP **07** (2013), 021 [arXiv:1302.1802 [hep-ph]].
- [20] C. B. Jackson, G. Servant, G. Shaughnessy, T. M. P. Tait and M. Taoso, JCAP **07** (2013), 006 [arXiv:1303.4717 [hep-ph]].
- [21] A. Delgado, A. Martin and N. Raj, Phys. Rev. D **95**, no.3, 035002 (2017) [arXiv:1608.05345 [hep-ph]].
- [22] R. T. D'Agnolo and J. T. Ruderman, Phys. Rev. Lett. **115** (2015) no.6, 061301 [arXiv:1505.07107 [hep-ph]].
- [23] R. T. D'Agnolo, D. Liu, J. T. Ruderman and P. J. Wang, JHEP **06** (2021), 103 [arXiv:2012.11766 [hep-ph]].
- [24] G. N. Wojcik and T. G. Rizzo, JHEP **04**, 033 (2022) [arXiv:2109.07369 [hep-ph]].
- [25] J. Herms, S. Jana, V. P. K. and S. Saad, Phys. Rev. Lett. **129**, no.9, 9 (2022) [arXiv:2203.05579 [hep-ph]].
- [26] K. C. Yang, JHEP **11**, 083 (2022) [arXiv:2209.10827 [hep-ph]].
- [27] Y. Liu, X. Liu and B. Zhu, Phys. Rev. D **107**, no.11, 11 (2023) [arXiv:2301.12199 [hep-ph]].
- [28] A. Aboubrahim, M. Klasen and L. P. Wiggering, [arXiv:2306.07753 [hep-ph]].
- [29] Y. Cheng, S. F. Ge, J. Sheng and T. T. Yanagida, Phys. Rev. D **107**, no.12, 123013 (2023) [arXiv:2304.02997 [hep-ph]].
- [30] K. C. Yang, JHEP **11** (2019), 048 [arXiv:1905.09582 [hep-ph]].
- [31] R.L. Workman et al. (Particle Data Group), Prog. Theor. Exp. Phys. 2022, 083C01 (2022).
- [32] S. Baek, P. Ko, W. I. Park and E. Senaha, JHEP **05**, 036 (2013) [arXiv:1212.2131 [hep-ph]], and references therein.
- [33] A. V. Artamonov *et al.* [BNL-E949], Phys. Rev. D **79**, 092004 (2009) [arXiv:0903.0030 [hep-ex]].
- [34] D. Gorbunov, I. Krasnov and S. Suvorov, Phys. Lett. B **820**, 136524 (2021) [arXiv:2105.11102 [hep-ph]].
- [35] F. Bergsma *et al.* [CHARM], Phys. Lett. B **157**, 458-462 (1985)
- [36] M. W. Winkler, Phys. Rev. D **99**, no.1, 015018 (2019) [arXiv:1809.01876 [hep-ph]].
- [37] M. Acciarri *et al.* [L3], Phys. Lett. B **385**, 454-470 (1996)
- [38] S. Alekhin, W. Altmannshofer, T. Asaka, B. Batell, F. Bezrukov, K. Bondarenko, A. Boyarsky, K. Y. Choi, C. Corral and N. Craig, *et al.* Rept. Prog. Phys. **79**, no.12, 124201 (2016) [arXiv:1504.04855 [hep-ph]].
- [39] C. Ahdida *et al.* [SHiP], JINST **14**, no.03, P03025 (2019) [arXiv:1810.06880 [physics.ins-det]].
- [40] E. Cortina Gil *et al.* [NA62], JINST **12**, no.05, P05025 (2017) [arXiv:1703.08501 [physics.ins-det]].
- [41] K. Bondarenko, A. Boyarsky, T. Bringmann, M. Hufnagel, K. Schmidt-Hoberg and A. Sokolenko, JHEP **03**, 118 (2020) [arXiv:1909.08632 [hep-ph]].

- [42] N. Aghanim *et al.* [Planck], *Astron. Astrophys.* **641**, A6 (2020) [Erratum: *Astron. Astrophys.* **652**, C4 (2021)] [arXiv:1807.06209 [astro-ph.CO]].
- [43] G. Mangano, G. Miele, S. Pastor, T. Pinto, O. Pisanti and P. D. Serpico, *Nucl. Phys. B* **729**, 221-234 (2005) [arXiv:hep-ph/0506164 [hep-ph]].